Dehalogenation of Chloroalkenes at Cobalt Centers. A Model Density Functional Study

Michael Bühl,*,† Ivana Vinković Vrček,‡ and Hendrik Kabrede†

Max-Planck-Institut für Kohlenforschung, Kaiser-Wilhelm-Platz 1, D-45470 Mülheim an der Ruhr, Germany, and Faculty of Pharmacy and Biochemistry, University of Zagreb, HR-10000, Zagreb, Croatia

Received January 11, 2007

Reaction of a model cobaloxime, $MeCo(Hgly)_2(NHCH_2)$ (Hgly = glyoximato), with chloro ethenes $ClX_1C{=}CX_2X_3$ (X = Cl or H) under reductive conditions has been investigated at the BP86 level of density functional theory. Initial one-electron reduction of the metal complex affords either $[MeCo(Hgly)_2]^{\bullet-}$ or $[Co(Hgly)_2(NHCH_2)]^-$. Both can react with the substrates under chloride elimination to form the corresponding vinylcobalt complexes with a $Co-CX_1{=}CX_2X_3$ moiety, which is indicated to be the rate-limiting step in a potential catalytic cycle. Free energies of activation on the order of 20 kcal/mol are predicted for these processes, suggesting that such an inner-sphere reduction (i.e., one that takes place in the coordination sphere of the metal) could be a viable pathway. Implications for the mechanism with functional biological systems based on vitamin B_{12} are discussed.

1. Introduction

Ever since their introduction as simple vitamin B_{12} model complexes four decades ago,[1] cobaloximes have attracted the interest of chemists and continue to do so.[2,3] A recent intriguing aspect, for instance, is that cobaloximes can be active electrocatalysts for proton reduction, mimicking the function of hydrogenases.[3] Cobaloxime complexes have also been used to model putative intermediates involved in the B_{12}-catalyzed reductive dehalogenation of chloroalkenes.[4] This reaction (sketched in Scheme 1) was discovered in the 1990s[5] and is now recognized as one of the many facets of the chemistry of vitamin B_{12}.[6] Driven by the environmental problems posed by halogenated pollutants and by the potential opportunity of their detoxification with bioinspired "Green Chemistry" methods, numerous studies have been directed at elucidating the mechanism of this catalytic process.[7−13]

In the presence of a stochiometric, sacrificial reducing agent, such as Ti^{III}, cob(I)alamin (Cbl^I) is believed to be the key species in the catalytic cycle. Itself both a strong reductant and nucleophile,[14] Cbl^I could either reduce the chloroalkene directly via an outer-sphere mechanism or be involved in more "intimate interactions" with the substrate, up to the point where the latter enters the coordination sphere of the metal. Evidence for such a scenario has recently been provided by kinetic modeling of concerted and stepwise pathways.[7] The successful isolation of chlorinated vinyl cobaloxime[4] and cobalamine complexes[15] would also be consistent with such an inner-sphere mechanism, in the course of which these vinyl cobalt complexes could be formed as reactive intermediates. Another route involving chlorinated alkylcobalt species has been proposed recently.[13] Despite all these efforts, the precise mechanism of catalysis is not yet fully understood.

Quantum chemical (ab initio or density functional) methods have already been used to shed light on various aspects of the chemistry involved in reductive dehalogenation of chloroethylenes. For instance, the fate of reduced chloroethylenes (as they would emerge from outer-sphere reduction) has been studied in detail,[16] and computed structural, energetic, and electrochemical properties of chlorinated vinyl-[17] and alkylcobalamins[13] have been helpful in the interpretation of

* Corresponding author. Fax: 49-208-306-2996. E-mail: buehl@mpi-muelheim.mpg.de.

† Max-Planck-Institut für Kohlenforschung.

‡ University of Zagreb.

(1) (a) Schrauzer, G. N. *Acc. Chem. Res.* **1968**, *1*, 97−103. (b) Bresciani-Pahor, N.; Forcolin, M.; Marzilli, L. G.; Randaccio, L.; Summers, M. F.; Toscano, P. J. *Coord. Chem. Rev.* **1985**, *63*, 1−125.

(2) For some recent examples, see: (a) Gupta, B. D.; Yamuna, R.; Mandal, D. *Organometallics* **2006**, *25*, 706−7014. (b) Mandal, D.; Gupta, D. B. Eur. *J. Inorg. Chem.* **2006**, 4086−4095. (c) Siega, P.; Randaccio, L.; Marzilli, P. A.; Marzilli, L. G. *Inorg. Chem.* **2006**, *45*, 3359−3368. (d) Pidaparthi, R. R.; Welker, M. E.; Day, C. S. *Organometallics* **2006**, *25*, 974−981. Fritsch, J. M.; Retka, N. D.; McNeill, K. *Inorg. Chem.* **2006**, *45*, 2288−2295.

(3) (a) Hu, X.; Cossairt, B. M.; Brunschwig, B. S.; Lewis, N. S.; Peters, J. C. *Chem. Commun.* **2005**, 4723−4725. (b) Razavet, M.; Artero, V.; Fontecave, M. *Inorg. Chem.* **2005**, *44*, 4786−4795.

(4) (a) Rich, A. E.; DeGreeff, A. D.; McNeill, K. *Chem. Commun.* **2002**, 234−235. (b) McKauley, K. M.; Wilson, S. R.; van der Donk, W. A. *Inorg. Chem.* **2002**, *41*, 393−404.

(5) Gantzer, C. J.; Wackett, L. P. *Environ. Sci. Technol.* **1991**, *25*, 715−722.

(6) Brown, K. L. *Chem. Rev.* **2005**, *105*, 2075−2149.

(7) (a) Lesage, S.; Brown, S.; Millar, K. *Environ. Sci. Technol.* **1998**, *32*, 2264−2272. (b) Glod, G.; Angst, W.; Hollinger, C.; Schwarzenbach, R. P. *Environ. Sci. Technol.* **1997**, *31*, 253−260. (c) Glod, G.; Brodmann, U.; Angst, W.; Hollinger, C.; Schwarzenbach, R. P. *Environ. Sci. Technol.* **1997**, *31*, 3154−3160.

(8) Costentin, C.; Robert, M.; Savéant, J.-M. *J. Am. Chem. Soc.* **2005**, *127*, 12154−12155.

(9) Burris, D. R.; Delcomyn, C. A.; Smith, M. H.; Roberts, A. L. *Environ. Sci. Technol.* **1996**, *30*, 3047−3052.

(10) For analogous dechlorination of alkyl halides, see, for example: Argüello, J. E.; Costentin, C.; Griveau, S.; Saveant, J.-M. *J. Am. Chem. Soc.* **2005**, *127*, 5049−5055, and references therein.

(11) Fritsch, J. M.; McNeill, K. *Inorg. Chem.* **2005**, *44*, 4852−4861.

(12) Follett, A. D.; McNeill, K. *J. Am. Chem. Soc.* **2005**, *127*, 844−845.

(13) Pratt, D. A.; van der Donk, W. A. *Chem. Commun.* **2006**, 558−560.

(14) Liptak, M. D.; Brunold, T. C. *J. Am. Chem. Soc.* **2006**, *128*, 9144−9156.

(15) (a) McKauley, K. M.; Wilson, S. R.; van der Donk, W. A. *J. Am. Chem. Soc.* **2003**, *125*, 4410−4411. (b) McKauley, K. M.; Pratt, D. A.; Wilson, S. R.; Shey, J.; Burkey, T. J.; van der Donk, W. A. *J. Am. Chem. Soc.* **2005**, *127*, 1126−1136.

(16) Nonnenberg, C.; van der Donk, W. A.; Zipse, H. *J. Phys. Chem. A* **2002**, *106*, 8708−8715.

10.1021/om070027s CCC: $37.00
Publication on Web 02/17/2007

Scheme 1

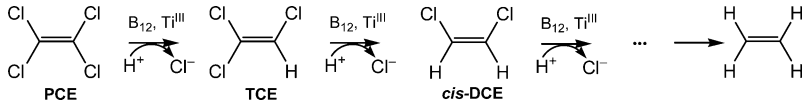

experimental observations. We were interested in the corresponding characteristics of simpler cobaloxime model complexes, calling special attention to thermodynamic driving forces and reaction barriers for addition of chloroethylenes to the metal center.

The purpose of this paper is twofold: First, with a potential development of cobaloxime complexes into biomimetic models for cobalamins and vitamin B_{12} in mind, we explore computationally key steps of the reaction between cobaloximes and chloroethylenes under reductive conditions. In case no substantial thermodynamic or kinetic hindrance would be revealed for the key steps in a potential catalytic cycle, functional models could perhaps be designed rationally by appropriate ligand tuning or identified by combinatorial synthesis and high-throughput screening. Second, detailed insights into the interaction between the reduced model complexes and the chloroethylene substrates can also have important implications for the mechanism of the actual vitamin B_{12}-catalyzed process. In keeping with recent experimental evidence that this reaction may not involve simple outer-sphere reduction,[12] we now present computational results illustrating what a viable inner-sphere pathway could look like.

2. Computational Details

Geometries were fully optimized at the RI-BP86/AE1 level, i.e., employing the exchange and correlation functionals of Becke[18] and Perdew,[19] respectively, together with a fine integration grid (75 radial shells with 302 angular points per shell), the augmented Wachters' basis[20] on Co (8s7p4d, full contraction scheme 62111111/3311111/3111), 6-31G* basis[21] on all other elements, and suitable auxiliary basis sets for the fitting of the Coulomb potential.[22] This and comparable DFT levels have proven quite successful for transition-metal compounds and are well suited for the description of structures, energies, barriers, and other properties.[23,24] Singlet and doublet states were described with the restricted and unrestricted Kohn−Sham formulation, respectively. Spin contamination in the latter calculations was small throughout, with $\langle \hat{S}^2 \rangle$ values not exceeding 0.76. Harmonic frequencies were computed analytically and were used without scaling to obtain enthalpic and entropic corrections. Refined energies were obtained from single-point calculations at the RI-BP86/AE2 level, employing the RI-BP86/AE1 geometries and 6-311+G* basis[25] (instead of 6-31G*) on the non-hydrogen atoms of the ligands. Unless otherwise noted, energies, ΔE, are reported at that level. With the same AE2 basis and RI-BP86/AE1 geometries, single-point energy calculations were also performed using the polarizable continuum model (PCM) of Tomasi and co-workers[26] (employing UFF radii scaled by 1.2 and the parameters of THF and water). The resulting energies ΔE with the AE2 basis (in vacuo or in the continuum) were corrected for the gas-phase enthalpic and entropic contributions (at the RI-BP86/AE1 level), to afford estimates for ΔH and ΔG. In selected cases, the corresponding single points were also evaluated at the B3LYP/AE2 level, that is, using the functionals according to Becke (hybrid)[27] and Lee, Yang, and Parr.[28] Atomic charges and spin densities were evaluated from natural population analysis (NPA)[29] at the PCM(H_2O)/BP86/AE2 level.

Reduction potentials, E^0, relative to the standard hydrogen electrode (SHE) were evaluated from gas-phase electron affinities, ΔE^{EA}, obtained from the RI-BP86/AE2 single points,[30] corrections to ΔG^{EA} from the RI-BP86/AE1 level, and differential solvation free energies, ΔG^S, from PCM single points in water, according to $E^0 = -(\Delta G^{EA} + \Delta G^S)/nF + E^0_{SHE}$, where n is the number of electrons (1 in our case), F is the Faraday constant (23.061 kcal mol^{-1} V^{-1}), and E^0_{SHE} is the reduction potential of the SHE ($E^0_{SHE} = -4.36$ V[31]), cf. the protocol of Truhlar and co-workers.[32] A similar approach has been used previously to compute reduction potentials of chloroethylenes and vinylcobalamin models.[17] All computations employed the Gaussian 03 program package.[33]

3. Results and Discussion

Our simplest cobaloxime model with a coordinated nitrogen base, MeCo(Hgly)$_2$($NHCH_2$) (**1**) (Hgly = glyoximato), is depicted in Chart 1.

The BP86-optimized Co−C bond length of **1**, 2.008 Å, is in excellent agreement with that observed for the corresponding pyridine adduct in the solid, 2.005 Å,[34] and close to those in other B_{12} models, e.g., 1.986 Å in MeCo(HDmg)$_2$(Im) (dmg = dimethylglyoximato, Im = imidazole),[35] or in

(17) Pratt, D. A.; van der Donk, W. A. *J. Am. Chem. Soc.* **2005**, *127*, 384−396.
(18) Becke, A. D. *Phys. Rev. A* **1988**, *38*, 3098−3100.
(19) (a) Perdew, J. P. *Phys. Rev. B* **1986**, *33*, 8822−8824. (b) Perdew, J. P. *Phys. Rev. B* **1986**, *34*, 7406.
(20) (a) Wachters, A. J. H. *J. Chem. Phys.* **1970**, *52*, 1033−1036. (b) Hay, P. J. *J. Chem. Phys.* **1977**, *66*, 4377−4384.
(21) (a) Hehre, W. J.; Ditchfield, R.; Pople, J. A. *J. Chem. Phys.* **1972**, *56*, 2257−2261. (b) Hariharan, P. C.; Pople, J. A. *Theor. Chim. Acta* **1973**, *28*, 213−222.
(22) Generated automatically according to the procedure implemented in Gaussian 03.
(23) See for instance: Koch, W.; Holthausen, M. C. *A Chemist's Guide to Density Functional Theory*; Wiley-VCH: Weinheim, 2000.
(24) In particular as far as geometries of transition-metal complexes are concerned, the popular B3LYP functional need not be superior to pure, gradient-corrected variants such as BP86; see for instance: (a) Hamprecht, F. A. H.; Cohen, A. J.; Tozer, D. J.; Handy, N. C. *J. Chem. Phys.* **1998**, *109*, 6264−6271. (b) Barden, C. J.; Rienstra-Kiracofe, J. C.; Schaefer, H. F. *J. Chem. Phys.* **2000**, *113*, 690−700. (c) Bühl, M.; Kabrede, H. *J. Chem. Theor. Comput.*, in press.
(25) (a) Krishnan, R.; Binkley, J. S.; Seeger, R.; Pople, J. A. *J. Chem. Phys.* **1980**, *72*, 650−654. (b) Clark, T.; Chandrasekhar, J.; Spitznagel, G. W.; Schleyer, P. v. R. *J. Comput. Chem.* **1983**, *4*, 294−301.
(26) As implemented in G 03: (a) Barone, V.; Cossi, M.; Tomasi, J. *J. Comput. Chem.* **1998**, *19*, 404−417. (b) Cossi, M.; Scalmani, G.; Rega, N.; Barone, V. *J. Chem. Phys.* **2002**, *117*, 43−54. (c) Cossi, M.; Crescenzi, O. *J. Chem. Phys.* **2003**, *19*, 8863−8872.
(27) Becke, A. D. *J. Chem. Phys.* **1993**, *98*, 5648−5642.
(28) Lee, C.; Yang, W.; Parr, R. G. *Phys. Rev. B* **1988**, *37*, 785−789.
(29) Reed, A. E.; Curtiss, L. A.; Weinhold, F. *Chem. Rev.* **1988**, *88*, 899−926.
(30) For a review on theoretical computations of electron affinities see: Rinstra-Kiracofe, J. C.; Tschumper, G. S.; Schaefer, H. F., III. *Chem. Rev.* **2002**, *102*, 231−282.
(31) Lewis, A.; Bumpus, J. A.; Truhlar, D. G.; Cramer, C. J. *J. Chem. Educ.* **2004**, *81*, 596−604.
(32) Winget, P.; Cramer, C. J.; Truhlar, D. G. *Theor. Chem. Acc.* **2004**, *112*, 217−227.
(33) Frisch, M. J.; et al. *Gaussian 03*; Gaussian, Inc.: Pittsburgh, PA, 2003.
(34) Bresciani-Pahor, N.; Randaccio, L.; Zangrando, E.; Toscano, P. J. *Inorg. Chim. Acta* **1985**, *96*, 193−198.
(35) Patthabi, V.; Nethaji, M.; Gabe, E. J.; Lee, F. L.; Le, Page, Y. *Acta Crystallogr. Sect. C* **1984**, *40*, 1155.

Chart 1

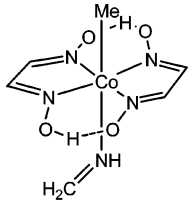

1

MeCbl^{III} itself, 1.99(2) Å.[36] The Co−C bond dissociation enthalpy (BDE) of **1**, eq 1,

$$\mathbf{1} \rightarrow [\mathrm{Co(Hgly)_2(NHCH_2)}]^{\bullet}\ (\mathbf{2}) + \mathrm{Me}^{\bullet} \qquad (1)$$

is computed to be 40.7 kcal/mol (ΔH at the BP86 level), somewhat higher than that computed for MeCbl^{III} (35.9 kcal/mol using the same functional and a similar basis set)[37] or estimated from kinetic and electrochemical measurements for this coenzyme, 37 ± 3[38] and 31 ± 2 kcal/mol,[39] respectively. Even though the Co−C bond in **1** appears to be noticeably stronger than that in cobalamins, the simple cobaloxime should be a reasonably good qualitative model for the organometallic chemistry of complexes related to vitamin B_{12}, in particular when the considerable experimental uncertainty concerning the salient BDE is taken into account. The quantitative differences between cobaloximes and cobalamines in terms of electronic and structural properties, on the other hand, are well appreciated nowadays.[40]

The remainder of this section is organized as follows: First, the possible decomposition reactions of **1** after initial one-electron reduction are investigated. Second, we study the interactions of chloroalkenes with the reactive intermediate resulting from the more favorable process, which, as it turns out, is cleavage of the Co−imine bond. Finally, we discuss the analogous interactions involving the "base-on" reduced form of **1** after Co−C cleavage, attempting to model the corresponding chemistry of cobalamines.

3.1. Reduction of the Glyoximato Model. One-electron reduction of model complex **1** is indicated to be facile. In keeping with the observation that at the BP86 level (also at B3LYP) the LUMO energy in **1** is negative, reduction to **1**$^{\bullet-}$ is exothermic in the gas phase, $\Delta E = -29.0$ kcal/mol at BP86. Because of the change in charge during this process, large solvation effects are to be expected. Typical solvents used in the experiments are THF and water (the latter usually with admixtures of ethanol or THF to increase solubility of the organic substrates). Results from simple single-point PCM calculations employing the parameters of these solvents (including thermal and entropy corrections from computations of gas-phase harmonic frequencies) are summarized in Table 1.

Table 1. Potential and Free Energies for Reduction of 1 to 1$^{\bullet-}$, Computed at Various DFT Levels [in kcal/mol], Together with Estimated Reduction Potentials E^0 [in V]

level[a]	phase	ΔE	ΔG	E^0
BP86	gas	−29.0	−34.0	
	THF	−60.1	−65.1[b]	−1.54
	H_2O	−64.8	−69.8[b]	−1.33
B3LYP	gas	−27.0	−32.0	
	THF	−57.5	−62.5[b]	−1.65
	H_2O	−62.0	−67.0[b]	−1.45

[a] Single-point calculations employing AE2 basis and geometries optimized at the BP86/AE1 level in the gas phase. [b] Thermal and entropic corrections obtained at the BP86/AE1 level in the gas phase.

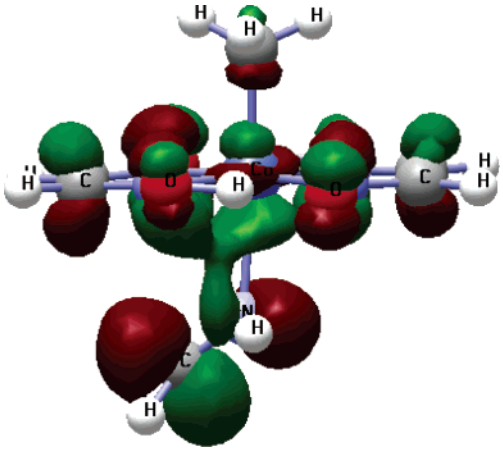

Figure 1. SOMO of **1**$^{\bullet-}$ (BP86/AE1 level).

As expected, solvation is indicated to stabilize the anion considerably, roughly doubling the driving force for reduction. Compared to the gas-phase values, changes between PCM results for THF and water are not very pronounced. Even smaller differences are encountered when switching from the pure GGA functional BP86 to the B3LYP hybrid functional. Similar findings were made in most of our subsequent calculations. In this paper we report values obtained at one representative level, BP86(H_2O). We note that the computed reduction potentials of **1** are in good qualitative accord with that reported for MeCo(HDmg)$_2$(Me$_3$Bzm) (Bzm = benzimidazole), −1.45 V.[40a]

In the radical anion, the bond between Co and the nitrogen donor is significantly weakened. This weakening is apparent from an elongation of the Co−N bond to the imine (from 1.983 Å in **1** to 2.212 Å in **1**$^{\bullet-}$), concomitant with a noticeable tilt of the imine plane away from the Co−N axis. In the singly occupied MO (SOMO) the odd electron is distributed over all the cobaloxime and imine moieties, with a clearly antibonding interaction between Co and N(imine); see Figure 1.

It is therefore not surprising that the bond energy (cf. eq 2) is very small, almost negligible in the gas phase (computed BDE 1.9 kcal/mol), and that the imine is essentially unbound when solvation and entropic effects are taken into account ($\Delta G(H_2O) = -12.4$ kcal/mol).

$$\mathbf{1}^{\bullet-} \rightarrow [\mathrm{MeCo(Hgly)_2}]^{\bullet-}\ (\mathbf{3}^{\bullet-}) + \mathrm{NHCH_2} \qquad (2)$$

Loss of the imine will thus be rapid in solution, so that the actual reduction process should be formulated as

$$\mathbf{1} + e^- \rightarrow \mathbf{3}^{\bullet-} + \mathrm{NHCH_2} \qquad (3)$$

(36) Rossi, M.; Glusker, J. P.; Randaccio, L.; Summers, M. F.; Toscano, P. J.; Marzilli, L. G. *J. Am. Chem. Soc.* **1985**, *107*, 1729−1738.

(37) There is also recent evidence from CASSCF calculations that DFT overestimates the Co−C BDE in methylcobalamin models: (a) Spataru, T.; Birke, R. L. *J. Phys. Chem. A* **2006**, *110*, 8599−8604. On the other hand, the BP86 functional has recently been shown to perform quite well in that respect: (b) Kuta, J.; Patchkovskii, S.; Zgierski, M. Z.; Kozlowski, P. *J. Comput. Chem.* **2006**, *27*, 1429−1437.

(38) Martin, B. D.; Finke, R. G. *J. Am. Chem. Soc.* **1992**, *114*, 585−592.

(39) Birke, R. L.; Huang, Q.; Spataru, T.; Gosser, T. K., Jr. *J. Am. Chem. Soc.* **2006**, *128*, 1922−1936. The entropic contribution inferred in that study, TDS = 13.6 ± 1.5 kcal/mol at 293 K, compares favorably to that computed for the process in eq 1, 14.0 kcal/mol (in contrast, much smaller entropic effects have been found in ref 38, TDS = 7 ± 2 kcal/mol at 293 K).

(40) See for example: (a) Randaccio, L.; Furlan, M.; Geremia, S.; Slouf, M.; Srnova, I.; Toffoli, D. *Inorg. Chem.* **2000**, *39*, 3403−3413. (b) Randaccio, L.; Geremia, S.; Nardin, G.; Wuerges, J. *Coord. Chem. Rev.* **2006**, *250*, 1332−1350.

Chart 2

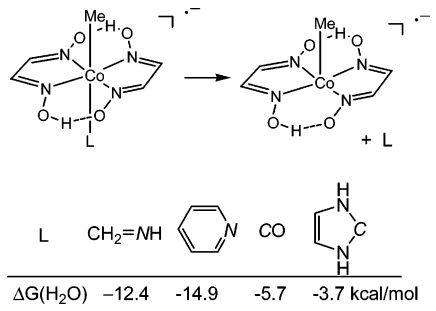

for which a large driving force is obtained, namely, $\Delta G(H_2O) = -82.3$ kcal/mol. This value corresponds to an estimated reduction potential of $E^0 = -0.79$ V, so that mild reducing agents such as Ti(III) complexes (experimental E^0 values between ca. -0.6 and -0.8 V)[41] could accomplish this initial reduction step.

In contrast, decay of $\mathbf{1}^{\bullet-}$ by loss of the methyl group is much less favorable, for both homolytic and heterolytic cleavage of the Co−C bond. Both processes are computed to be endergonic, with $\Delta G(H_2O) = 5.4$ and 28.4 kcal/mol for the reactions specified in eqs 4 and 5:

$$\mathbf{1}^{\bullet-} \rightarrow [Co(Hgly)_2(NHCH_2)]^- (\mathbf{2}^-) + Me^{\bullet} \qquad (4)$$

$$\mathbf{1}^{\bullet-} \rightarrow [Co(Hgly)_2(NHCH_2)]^{\bullet} (\mathbf{2}^{\bullet}) + Me^- \qquad (5)$$

This type of chemistry is typical for cobalamins and methylvitamin B_{12} itself. To what extent the base in these systems, dimethylbenzimidazole tethered to the corrin ring around Co, retains its coordination to the metal is unclear. Occurrence of "base-off" intermediates, where this coordination is temporarily broken, is frequently invoked for reactive intermediates believed to be central to the chemistry of the cofactor.[42] In our model system, homolytic Co−C cleavage (eq 4) is predicted to be strongly favored over heterolytic cleavage. The very small free energy for the former process, ca. 5 kcal/mol, is noteworthy. It should be kept in mind, however, that a large part of the driving force in that reaction stems from the gain in entropy due to the increase in particle number, as computed in the gas phase. The actual entropy effects in solution are probably less pronounced. Nevertheless, the Co−C bond in $\mathbf{1}^{\bullet-}$ is weak, with a computed BDE of 21.1 kcal/mol (eq 4, BP86/AE1 in the gas phase).

However, in our model complex the bond to the imine is even weaker. In order to probe whether potentially stronger donors could eventually be competitive with the Co−C bond in the radical anion, we optimized a few derivatives of **1** and $\mathbf{1}^{\bullet-}$, replacing the imine with pyridine, CO, and imidazol-2-ylidene, as a model for an N-heterocyclic carbene (NHC) ligand. The latter two ligands were chosen because of potential back-bonding from the metal to the ligand, which might lead to a reinforcement of the bond. In particular NHCs have recently emerged as promising ligands for many areas of transition metal chemistry.[43] However, none of these ligands are predicted to remain coordinated in the radical anion (cf. the ΔG values in Chart 2).

Thus, according to these results, reduction of cobaloxime complexes should result in loss of the ancillary ligand L, whereas cobalamines are likely to lose the metal-bonded alkyl group. In our model system, the two scenarios would correspond to the production of $\mathbf{3}^{\bullet-}$ and $\mathbf{2}^-$, respectively. Subsequently, we studied the reactions of both intermediates with chloroalkenes, calling special attention to the possibility of direct ("inner-sphere") reduction of the latter by the metal complexes. Results of these two reaction branches are discussed separately in the following.

3.2. Reaction of the "Base-Off" Model with Chloroalkenes. We first turn to the reactivity of the reduced "base-off" form $\mathbf{3}^{\bullet-}$ toward tetrachloroethene (PCE), which should model the corresponding chemistry of cobaloximes. In order to probe whether the metal complex could bind the olefin at its vacant coordination site, we constructed a suitable reaction coordinate, performing geometry optimizations of a $\mathbf{3}^{\bullet-}{\cdot}C_2Cl_4$ adduct with decreasing, fixed Co−C distances to the olefin. Indeed, these calculations indicated the presence of a minimum and transition state for its formation, which were subsequently located and characterized in full geometry optimizations (Figure 2). On the potential energy surface (PES) in the gas phase, the minimum $[MeCo(Hgly)_2(C_2Cl_4)]^{\bullet-}$ ($\mathbf{4}^{\bullet-}$) is 4.0 kcal/mol above the separated reactants, $\mathbf{3}^{\bullet-} + C_2Cl_4$, and is characterized by a fairly long Co−C bond to the olefin, 2.18 Å (much longer than the Co−C bond to the methyl group, 2.03 Å). With respect to the reactants, the transition state (**TS34**) is an early one, with a forming Co···C distance of 2.76 Å and an overall barrier of 6.0 kcal/mol.

Most significantly, in $\mathbf{4}^{\bullet-}$ one of the C−Cl bonds at the carbon attached to the metal is significantly elongated, to 1.99 Å (cf. 1.74 Å in C_2Cl_4). Apparently, this intermediate is already predisposed for rupture of this bond. In the gas phase, it costs only 0.4 kcal/mol to stretch this distance to 2.31 Å, at which point a transition state for dissociation of Cl^- is reached (**TS45**).[44] Salient energetic data for these stationary points are collected in Table 2. In the gas phase, the eventual product is an ion-dipole complex between Cl^- and $[MeCo(Hgly)_2(CCl=CCl_2)]^{\bullet}$ ($\mathbf{5}^{\bullet}$). Since this complex (which is not shown in Figure 2) is expected to be dissociated in solution, the energetic data of the separated products are included in Table 2.

As the liberation of chloride proceeds along the sequence $\mathbf{4}^{\bullet-} \rightarrow$ **TS45** $\rightarrow \mathbf{5}^{\bullet} + Cl^-$, stabilization in a polar solvent becomes more and more pronounced. Inclusion of such solvent effects brings the energy of **TS45** below that of $\mathbf{5}^{\bullet-}$, suggesting that the latter is not a stable intermediate in solution. Addition of the olefin via **TS34** is the highest point during this reaction. The activation barrier for this process is remarkably small, just 6.0−10.5 kcal/mol on the PES (ΔE values in Table 2). Assuming that the entropic penalty for this associative process will be smaller in solution than estimated from the gas-phase contributions included in $\Delta G(H_2O)$, the overall reaction

$$\mathbf{3}^{\bullet-} + C_2Cl_4 \rightarrow \mathbf{5}^{\bullet} + Cl^- \qquad (6)$$

should be feasible not only thermodynamically but also kinetically. This result, to our knowledge, is the first computational evidence that reductive cleavage of a C−Cl bond in a chlorinated alkene can be initiated by coordination to a cobalt center.

(41) (a) -0.63 V for Ti(III) chloride at pH 8; -0.70 V for the complex with ascorbate, cf. ref 7. (b) For Ti(III) citrate, an upper limit of -0.80 V has been estimated, cf. ref 17 in: Guo, M.; Sulc, F.; Ribbe, M. W.; Farmer, P. J.; Burgess, B. K. *J. Am. Chem. Soc.* **2002**, *124*, 12100−12101.

(42) Lexa, D.; Saveant, J.-M. *Acc. Chem. Res.* **1983**, *16*, 235−243.

(43) See for example: Crudden, C. M.; Allen, D. P. *Coord. Chem. Rev.* **2004**, *248*, 2247−2273, and references therein.

(44) That it is a chloride anion that is leaving, rather than a Cl radical, is apparent from population analyses, according to which the leaving Cl bears a charge of ca. $-0.4e$ (both from Mulliken and natural population analysis).

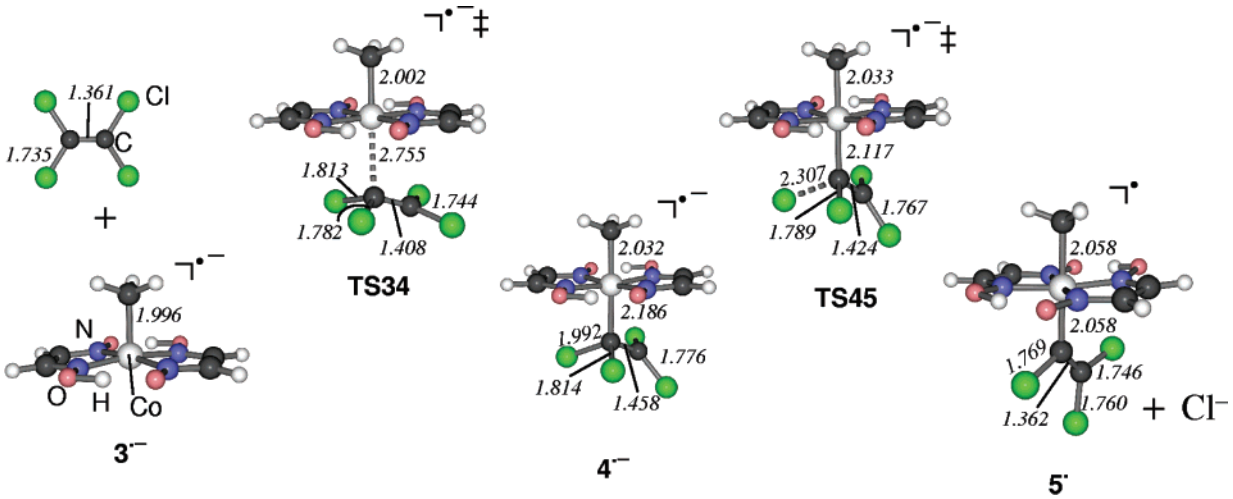

Figure 2. Stationary points for addition of PCE to $\mathbf{3}^{\bullet-}$ (in italics: selected BP86/AE1-optimized distances [in Å]).

Table 2. Relative Energies [kcal/mol] of Stationary Points with Respect to Separated Reactants $\mathbf{3}^{\bullet-} + C_2Cl_4$[a]

	TS34	$\mathbf{4}^{\bullet-}$	TS45	$\mathbf{5}^{\bullet} + Cl$
ΔE(gas)	6.0	4.0	4.4	20.0[b]
$\Delta E(H_2O)$	10.5	7.6	6.7	−7.2
$\Delta G(H_2O)$	22.8	21.8	21.1	−0.3

[a] BP86 level, AE2 single points on BP86/AE1-optimized geometries. [b] In the gas phase, a $\mathbf{6}^{\bullet}\cdot Cl^-$ complex is the product, with ΔE < 4.4 kcal/mol.

In our specific model system, the resulting vinyl complex $\mathbf{5}^{\bullet}$ should be quite reactive. It has a very high electron affinity ($\Delta G(H_2O)$ = −116.9 kcal/mol) and a positive reduction potential, E^0 = 0.71 V, suggesting that it will be readily converted to $\mathbf{5}^-$ under the reductive reaction conditions. Hydrolytic cleavage of the Co−C bond in $\mathbf{5}^-$ could then afford the first dehalogenation product, trichlorethylene (TCE), for instance after protonation:

$$\mathbf{5}^- + H_3O^+ \rightarrow \mathbf{3} + H_2O + CHCl{=}CCl_2 \qquad (7)$$

A large driving force, $\Delta G(H_2O)$ = −57.4 kcal/mol, is computed for this process, which could thus also be operative even in neutral solutions, i.e., at low concentrations of H_3O^+.

Other possibilities for decay of $\mathbf{5}^{\bullet}$ comprise reductive cleavage of Co−C bonds, e.g., according to

$$\mathbf{5}^{\bullet} + e^- \rightarrow \mathbf{3}^{\bullet-} + {}^{\bullet}CCl{=}CCl_2 \qquad (8)$$

which also has a notable driving force, $\Delta G(H_2O)$ = −79.3 kcal/mol (corresponding to E^0 = −0.92 V) and which would regenerate $\mathbf{3}^{\bullet-}$, thereby potentially closing a catalytic cycle. The trichlorovinyl radical produced in such a process would in turn be readily reduced (computed reduction potential E^0 = 0.50 V),[17] and the resulting trichlorovinyl anion rapidly protonated to afford TCE. Reductive Co−C cleavage according to

$$\mathbf{5}^{\bullet} + e^- \rightarrow \mathbf{3} + {}^{-}CCl{=}CCl_2 \qquad (9)$$

would even be more favorable, with $\Delta G(H_2O)$ = −97.3 kcal/mol (E^0 = −0.12 V). On this route, the neutral "base-off" variant **3** would be readily reduced (E^0 = −0.30 V) to restore the catalyst. Unfortunately, it is very difficult to compute reaction barriers for any of these processes. In view of the large driving forces, however, little kinetic hindrance is to be expected, and initial addition of PCE to $\mathbf{3}^{\bullet-}$ could well be the rate-determining step.

Next, we investigated the reaction of $\mathbf{3}^{\bullet-}$ with the first dehalogenation product, TCE. A relaxed scan, similar to that discussed above for $\mathbf{3}^{\bullet-} + C_2Cl_4$, gave a surprising result: at one point on the coordinate, when the CCl_2 group of TCE had approached the metal to 2.0 Å, a Cl atom from this group was spontaneously transferred to the other C atom, and the full geometry optimization starting from the point of lowest energy afforded the $[MeCo(Hgly)_2(CClCHCl_2)]^{\bullet-}$ complex ($\mathbf{6a}^{\bullet-}$, Figure 3) as stable minimum. Incidentally, the same minimum was obtained when a geometry optimization was started from the PCE adduct $\mathbf{4}^{\bullet-}$ after replacing one Cl atom of the "dangling" CCl_2 group with a H atom. When the other Cl atoms in $\mathbf{4}^{\bullet-}$ were substituted one after the other in a similar fashion, two additional isomers of $\mathbf{6a}^{\bullet-}$ were located (two of these optimizations converged to the same isomer); see plots in Figure 3. They all share the common feature of a strongly elongated C−Cl bond (dashed in Figure 3), predisposed for chloride dissociation. After dissociation of that chloride and hydrolysis of the Co−C bond (assuming retention of configuration at that C atom), $\mathbf{6a}^{\bullet-}$, $\mathbf{6b}^{\bullet-}$, and $\mathbf{6c}^{\bullet-}$ would afford *cis*-1,2-, 1,1-, and *trans*-1,2-dichloroethene (DCE), respectively. At the BP86/AE1 level, the relative energies of $\mathbf{6a}^{\bullet-}$, $\mathbf{6b}^{\bullet-}$, and $\mathbf{6c}^{\bullet-}$ are 0, 6.3, and 12.7 kcal/mol, respectively. Thus, if an inner-sphere mechanism involving these intermediates would be operative for our model complex, essentially exclusive formation of *cis*-1,2-DCE should occur at this stage.

It is interesting to note at this point that DCE produced during vitamin B_{12}-catalyzed dehalogenation of PCE is also predominantly the *cis*-1,2 isomer, together with small amounts of the other two forms. This product distribution has also been rationalized in terms of the stabilities of the corresponding dichloro-vinyl radicals, which would be intermediate products of outer-sphere reduction of the olefins, followed by chloride loss.[16]

The electronic structure of $\mathbf{6a}^{\bullet-}$ is interesting: the C(Cl)-$CHCl_2$ fragment would correspond to a carbene ligand,[45] and indeed the Co−C bond length to this moiety, 1.98 Å, is much shorter than that to the methyl group, 2.04 Å.[46] In contrast to formation of $\mathbf{4}^{\bullet-}$ from $\mathbf{3}^{\bullet-}$ + PCE, which is endothermic on all

(45) An attempted optimization of a corresponding $[MeCo(Hgly)_2(=CCl-CCl_3)]^{\bullet-}$ complex (which would be an isomer of $\mathbf{4}^{\bullet-}$) by replacing the H atom in $\mathbf{6a}^{\bullet-}$ with Cl resulted in chloride dissociation from the CCl_3 group, affording **5**.

(46) Formally, $\mathbf{6a}^{\bullet-}$ could be regarded as a Co(IV) species, a quite unusual oxidation state. For a recent paper on oxidized cobaloximes containing Co(IV) see: Ohkubo, K.; Fukuzumi, S. *J. Phys. Chem. A* **2005**, *109*, 1105−1113.

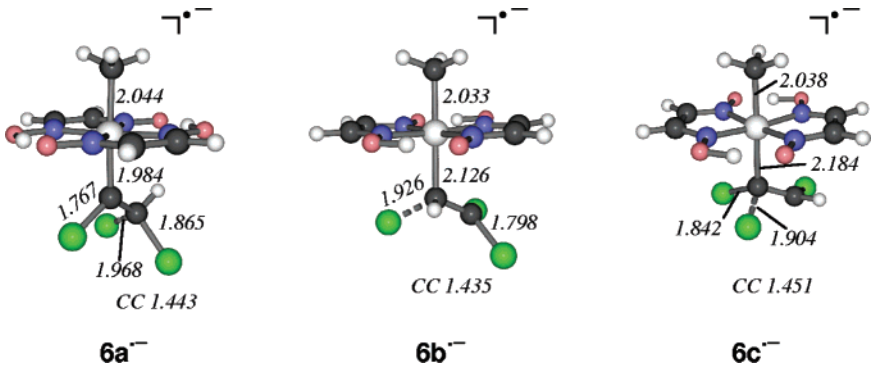

6a$^{\bullet-}$ **6b**$^{\bullet-}$ **6c**$^{\bullet-}$

Figure 3. Isomeric adducts of TCE to **3**$^{\bullet-}$ (in italics: selected BP86/AE1-optimized distances [in Å]).

levels (Table 2), addition of TCE to **3**$^{\bullet-}$ is slightly exothermic on the potential energy surface, as the computed ΔE values of **6a**$^{\bullet-}$ relative to these reactants are −4.1 and −0.1 kcal/mol in the gas phase and in water, respectively ($\Delta G(H_2O) = 14.4$ kcal/mol). We have not located the transition state leading to **6a**$^{\bullet-}$, but judging from the corresponding results for **4**$^{\bullet-}$, only slightly higher barriers are expected for this addition process (compare entries for **TS34** and **4**$^{\bullet-}$ in Table 2). The driving force for chloride loss and formation of the vinyl complex according to

$$\mathbf{3}^{\bullet-} + \text{TCE} \rightarrow [\text{MeCo(Hgly)}_2(\text{CCl=CHCl})]^{\bullet}\ (\mathbf{7}^{\bullet}) + \text{Cl}^- \quad (10)$$

is $\Delta G(H_2O) = -1.9$ kcal/mol, i.e., slightly more negative than that in eq 6 (−0.3 kcal/mol at the same level, Table 2). Thus, if reduction of chloroethenes can be initiated by coordination to the Co fragment, our model cobaloxime complexes are indicated to react faster with TCE than with PCE. On the other hand, the enhanced stability of **7**$^{\bullet}$ (as opposed to that of **5**$^{\bullet}$) would make its eventual decay somewhat less favorable, e.g., according to

$$\mathbf{7}^{\bullet} + e^- \rightarrow \mathbf{3}^{\bullet-} + \textit{cis}\text{-1,2-}^{\bullet}\text{CCl=CHCl} \quad (11)$$

The driving force of this reaction, $\Delta G(H_2O) = -75.7$ kcal/mol (corresponding to $E^0 = -1.08$ V), is less negative by 3.6 kcal/mol than that of eq 9. Whether that would lead to increased kinetic hindrance of a potential catalytic cycle in the case of TCE is hard to gauge at this point. In any event, the intermediate dichlorovinyl radical produced in eq 10 would be readily reduced (computed $E^0 = 0.31$ V) and, arguably, rapidly protonated. Overall, the reductive dechlorination of TCE should be possible with cobaloxime complexes, probably faster than that of PCE, and should afford predominantly the *cis*-1,2-DCE as product.

In the next step, we studied the reaction of this *cis*-1,2-DCE product with **3**$^{\bullet-}$. Interestingly, when we tried to locate the resulting olefin adduct **8**$^{\bullet-}$ (corresponding to **4**$^{\bullet-}$ and **6b**$^{\bullet-}$) by starting from the geometry of **4**$^{\bullet-}$ and replacing two Cl atoms with H, a stable minimum could only be found with loose thresholds for convergence of wave function and geometry optimization.[47] Reoptimization with the usual convergence criteria resulted in dissociation of DCE, affording a loose ion-dipole complex with **3**$^{\bullet-}$. Apparently, the addition of DCE to **3**$^{\bullet-}$ and loss of Cl$^-$ can occur without formation of a transient (shallow) minimum on the PES. Assuming that the transition-state region for this process is reasonably well modeled by the loosely optimized stationary point **8**$^{\bullet-}$, its energy should provide a rough estimate for the barrier that is involved. At the ΔE(gas) and $\Delta E(H_2O)$ levels, this barrier is computed to be 4.4 and 9.1 kcal/mol, respectively, that is, slightly higher than those computed for addition of PCE to **3**$^{\bullet-}$ (see corresponding ΔE values of **4**$^{\bullet-}$ in Table 2), but still on the same order of magnitude. However, the driving force for chloride loss and formation of the vinyl complex according to

$$\mathbf{3}^{\bullet-} + \text{DCE} \rightarrow [\text{MeCo(Hgly)}_2(\text{CH=CHCl})]^{\bullet}\ (\mathbf{9}^{\bullet}) + \text{Cl}^- \quad (12)$$

is $\Delta G(H_2O) = 7.1$ kcal/mol, significantly less favorable than the corresponding processes involving PCE and TCE (eqs 6 and 10, respectively). Dechlorination of DCE, if proceeding via an inner-sphere mechanism, would thus be expected to proceed slower than that of the higher chloroethylenes. The thermodynamic driving force for reductive decomposition of **9**$^{\bullet}$ yielding **3**$^{\bullet-}$ and $^{\bullet}$CH=CHCl is similar to that of the analogous process involving **5**$^{\bullet-}$ (eq 8), with $\Delta G(H_2O) = -77.5$ kcal/mol ($E^0 = -1.00$ V). The alternative pathway yielding **3** and $^-$CH=CHCl is not viable in this case, because the resulting chlorovinyl anion is unstable even in the gas phase, where it spontaneously dissociates into Cl$^-$ and acetylene (or, rather, into a weak H-bonded complex between both). This pathway would thus correspond to the overall reaction

$$\mathbf{9}^{\bullet} + e^- \rightarrow \mathbf{3} + \text{HC}\equiv\text{CH} + \text{Cl}^- \quad (13)$$

for which a large driving force is predicted, $\Delta G(H_2O) = -110.8$ kcal/mol ($E^0 = 0.45$ V), mainly due to the increase in particle number. A corresponding route could be responsible for the formation of acetylene, which has been observed during the B_{12}-catalyzed dehalogenation of PCE.[7a,9]

Finally, we studied the reaction of **3**$^{\bullet-}$ with CH_2=CHCl, vinyl chloride (VC), the eventual hydrolysis product of **9**$^{\bullet}$. In this case, no initial adduct between the reactants could be located at all. Coordination of the olefin under chloride loss and formation of the vinyl complex $[MeCo(Hgly)_2(CH=CH_2)]^{\bullet}$ (**10**$^{\bullet}$) proceeds in a single step. We have located the transition state for this process, **TS310**, which is analogous to **TS45** in Figure 2. Relative to the separated reactants and **3**$^{\bullet-}$, **TS310** is higher in energy by 16.4, 18.4, and 31.4 kcal/mol at the ΔE(gas), $\Delta E(H_2O)$, and $\Delta G(H_2O)$ levels, respectively. These values are much larger than the corresponding ones for **TS45** (or **TS34** or **4**$^{\bullet-}$) in Table 2, suggesting that formation of **10**$^{\bullet}$ via this path would be significantly hindered kinetically, if not prevented at all. Thus, if cobaloximes follow the inner-sphere mechanism we are discussing, reductive dehalogenation of DCE and, in particular, VC would proceed much slower than that of PCE and TCE. Salient energetic data for the lower chlorinated olefins are summarized in Table 3, for easy comparison with the results for **TS34** or **4**$^{\bullet-}$ in Table 2.

To summarize this section, we have provided computational evidence how simple cobaloxime complexes could mediate reductive dechlorination of PCE via an inner-sphere mechanism,

(47) Energy converged to 10^{-6} au and opt = loose keyword.

Table 3. Relative Energies [kcal/mol] of Stationary Points with Respect to Separated Reactants $3^{\bullet-}$ + Olefin as Indicated[a]

	olefin/stationary point		
	TCE/6a$^{\bullet-}$	***cis*-DCE/8$^{\bullet-}$** [b]	**VC/TS310**
ΔE(gas)	−4.1	4.4	16.4
$\Delta E(H_2O)$	−0.1	9.1	18.4
$\Delta G(H_2O)$	14.4	n.a.	31.4

[a] BP86 level, AE2 single points on BP86/AE1-optimized geometries. [b] Loosely optimized structure, see text (no frequencies computed, hence no enthalpic and entropic contributions).

at least to the DCE stage. This route is indicated to involve base-off alkylcobaloxime radicals as key species reacting with the substrates, i.e., following a mechanism completely different than that believed to be operative in the vitamin B_{12} system. Prediction of whether actual catalytic turnover could be achieved with these model systems appears to be difficult at this point. The absence of substantial kinetic hindrance in the elementary steps considered, however, would bestow some potential for further development of cobaloximes.

3.3. Reaction of the "Base-On" Model with Chloroalkenes. We now turn to the reactivity of the reduced "base-on" form **2**$^-$, the product of homolytic Co−C bond cleavage in **1**$^{\bullet-}$ (eq 4) toward PCE. As mentioned above, this reaction should model the corresponding chemistry of the cobalamins and, possibly, vitamin B_{12}. We were able to locate a transition state for addition of PCE to **2**$^-$ (**TS211** in Figure 4), leading directly to the vinyl complex **11** under loss of chloride. No other minima along that path that would correspond to, for example, **4**$^{\bullet-}$ (Figure 2) could be located. Attempts to perform a relaxed scan along one Co···C coordinate resulted in dissociation of the imine as the olefin approached.

The barrier for this route is quite high, however: on the potential energy surface, **TS211** is already ca. 15−19 kcal/mol above the reactants (Table 4) and is further disfavored by a substantial entropic penalty for this associative process. With the simple ideal-gas approximation, a free-energy barrier exceeding 30 kcal/mol is predicted for this path, clearly too high for a fast and efficient reaction.

It is noteworthy that in **TS211** the imine ligand appears to be quite loosely bound, with a very long Co−N distance of approximately 2.3 Å (Figure 4). Therefore, we investigated the dissociative pathway, initiated by loss of the imine ligand in **2**$^-$. The binding energy of the imine in **2**$^-$ is indeed quite low (only a few kcal/mol estimated on the free-energy surface, cf. the fourth column in Table 3), so that entry into this path should be possible. The resulting bare Co(I) fragment $[Co(Hgly)_2]^-$ (**12**$^-$)[48] readily takes up the olefin under formation of a η^2-bonded complex (or metallacycle), **13**$^-$.[49] No η^1-bonded minimum (corresponding to **4**$^{\bullet-}$ in Figure 2) could be located, and no transition state for separation of **13**$^-$ into free PCE and **12**$^-$ could be found. When the olefin is pulled away from the metal in **13**$^-$ in a relaxed scan, the energy rises continuously, approaching that of the fully separated products.

The olefin complex **13**$^-$ can lose a chloride ion under formation of the neutral vinyl derivative **14**. The barrier for this step, proceeding via transition state **TS13−14**, is slightly higher than that via **TS211** on the potential energy surface (see, for example, $\Delta E(H_2O)$ values in Table 4). Relative to the reactants PCE and **2**$^-$, however, no change in particle numbers occurs in **TS13−14**, so that the entropic correction is quite small in this case, and the predicted free-energy barrier via **TS13−14**, 19.7 kcal/mol, is much smaller than that via **TS211**, 32.5 kcal/mol. The former value is comparable to that computed for the methylated "base-off" variant in the preceding section (cf. **TS34** in Table 2). Thus, an inner-sphere mechanism could also be operative in dealkylated Co(I) complexes, but only in the "base-off" form.

Interestingly, the vinyl complex **14** has a quite pronounced affinity for binding of the imine, much higher than that of the Co(I) species **12**$^-$. In an inner-sphere pathway involving the real B_{12} catalyst, the flexibility of the base tethered to the corrin ring could be beneficial: conversion into the "base-off" form would facilitate substrate binding and reduction, after which recoordination of the base would provide additional thermodynamic driving force for this overall reaction step (see simplified sketch in Scheme 2).

For simple cobaloximes or other models with a free base, such an "on/off" switch mechanism is probably less favorable kinetically, because the fully liberated and dissociated base is not readily available and has to diffuse back to the metal center. Fast catalytic turnover would probably be particularly difficult in this case, because the concentration of the base necessary to provide the eventual driving force for the reaction would be low.

Once the vinyl complex **12** is formed, its Co−C bond would have to be cleaved reductively in order to complete the dehalogenation reaction. As with the actual reactant **1**, loss of the imine is more likely for the simple cobaloximes. However, there is also a notable driving force for the reaction

$$\mathbf{11} + e^- \rightarrow \mathbf{2}^{\bullet} + {}^-CCl{=}CCl_2 \qquad (14)$$

with computed $\Delta G(H_2O) = -82.0$ kcal/mol, corresponding to an estimated $E^0 = -0.80$ V. This reaction would eventually produce TCE. For a closely related derivative of **11**, *cis*-1,2-dichlorovinyl(pyridine)cobaloxime, the feasibilty of this reductive hydrolysis and the occurrence of chlorinated vinyl anions have recently been demonstrated.[50] Reduction of the Co(II) species **2**$^{\bullet}$ to **2**$^-$ (estimated $E^0 = -0.35$ V) would restore the anionic "base-on" complex for attack of new substrate. Again, computation of barriers or rate constants for these processes is difficult, but from the pronounced driving forces, little kinetic hindrance is to be expected. Thus, if PCE dehalogenation follows an inner-sphere mechanism involving dealkylated Co(I) complexes, it is likely that chloride dissociation in transient "base-off" olefin complexes will be the rate-limiting step, occurring via transition states resembling **TS13−14**. The computed free energy barrier for this process in our cobaloxime model suggests that this could indeed be a viable pathway.

Assuming that the basic underlying potential energy surface is qualitatively transferable to the other chlorinated ethylene derivatives, we finally investigated how this rate-determining barrier would change with the nature of the substrate. To this end, we successively replaced the vinylic Cl atoms in **TS13−14** with H atoms, affording the transition states displayed in Figure 5 and the relative energies collected in Table 5.

Eventually, after hydrolysis of the vinyl complex under retention at C, conversion of TCE via **TS15a**, **TS15b**, and **TS15c** would afford *cis*-1,2-, 1,1-, and *trans*-1,2-DCE, respectively. From the energies of the transition states in Table 4 it is

(48) The corresponding four-coordinate cob(I)alamin has been termed supernucleophile, cf. ref 14.

(49) There is structural precedence for an anionic, η^2-coordinated cobalt−olefin complex, $Li[Co(PMe_3)_3(C_2H_4)]$: Klein, H.-F.; Witty, H.; Schubert, U. *Chem. Commun*. **1983**, 231−232.

(50) Follett, A. D.; McNeill, K. *Inorg. Chem.* **2006**, *45*, 2727−2732.

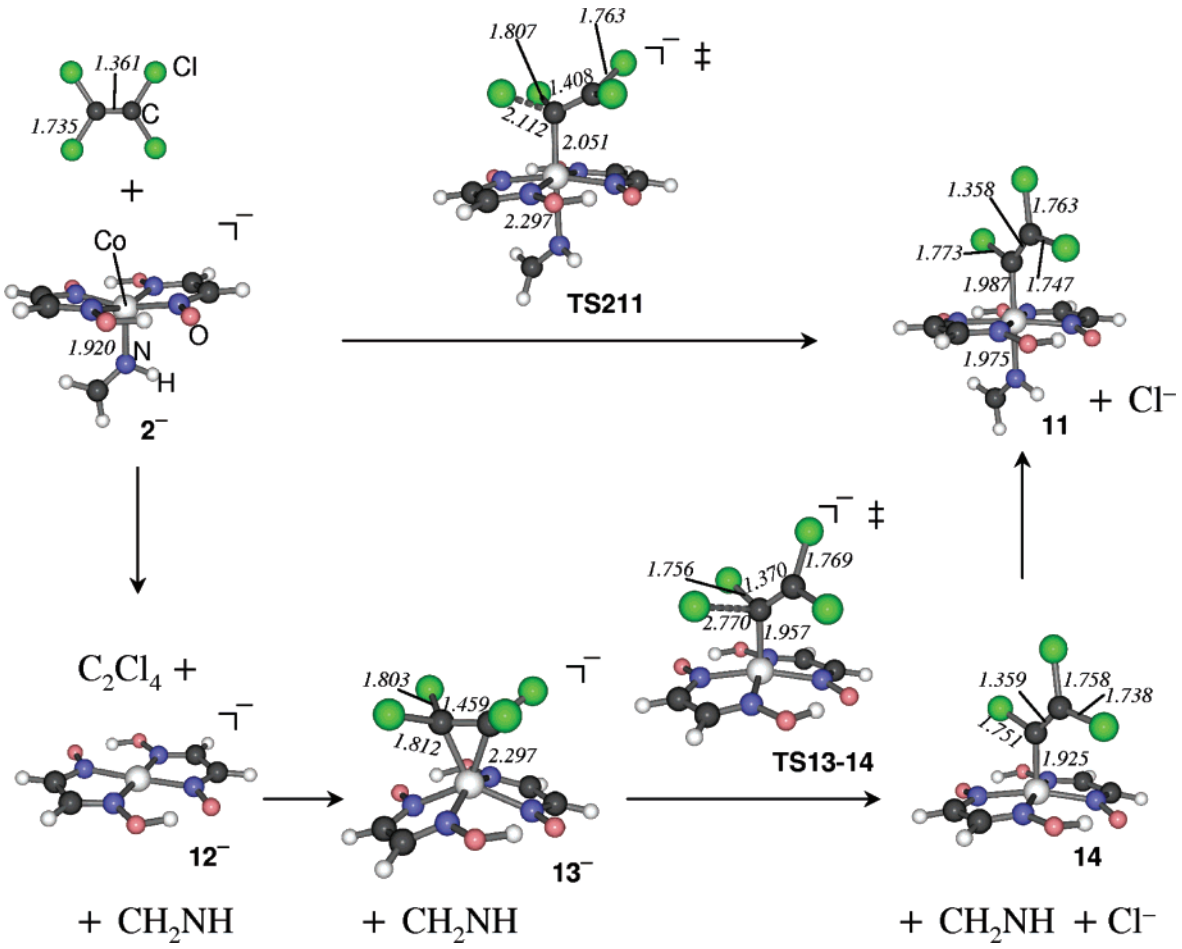

Figure 4. Stationary points for addition of PCE to $\mathbf{2}^-$ (in italics: selected BP86/AE1-optimized distances [in Å]).

Table 4. Relative Energies [kcal/mol] of Stationary Points with Respect to Separated Reactants $\mathbf{2}^- + \mathbf{C_2Cl_4}$[a]

	TS211	**11** + Cl^-	**12**$^-$+C_2Cl_4 + CH_2NH	**13**$^-$ + CH_2NH	**TS13−14** + CH_2NH	**14** + Cl^- + CH_2NH
ΔE(gas)	15.2	0.1	18.3	−8.8	20.3	31.2[b]
$\Delta E(H_2O)$	18.8	−26.7	17.7	−4.7	19.2	4.3
$\Delta G(H_2O)$	32.5	−18.2	4.3	−2.4	19.7	−2.2

[a] BP86 level, AE1+ single points on BP86/AE1-optimized geometries. [b] In the gas phase, a **14**·Cl^- complex is the product, with ΔE < 20.3 kcal/mol.

Scheme 2

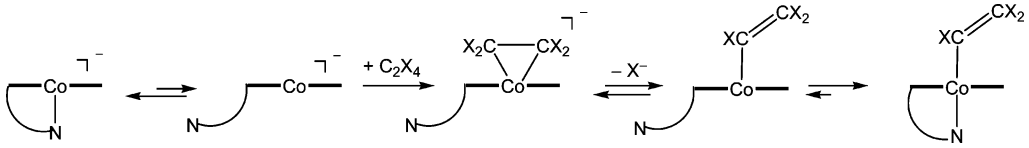

apparent that *cis*-1,2-DCE should be the principal product under kinetic control. This result is consistent with the product distribution of vitamin B_{12}-catalyzed dehalogenation of PCE, where it is also the *cis*-1,2 form that is predominately found among the isolated DCE isomers.[16] The product ratio of *cis*- and *trans*-1,2-DCE upon TCE reduction has recently been proposed as diagnostic for the underlying mechanism,[12] from which it has been concluded that outer-sphere reduction by vitamin B_{12} is unlikely to be the major pathway.

cis-1,2-DCE, *trans*-1,2-DCE, and their eventual dehalogenation product VC can further react via **TS16a**, **TS16b**, and **TS17**, respectively. For the different substrates, the computed activation barriers increase in the sequence TCE < PCE < *trans*-1,2-DCE < *cis*-1,2-DCE < VC (with ΔG values of 18.3, 19.7, 21.0, 25.6, and 26.7 kcal/mol for **TS15a**, **TS13**−**14**, **TS16b**, **TS16a**, and **TS17**, respectively). Except for the reversal of PCE and TCE, this trend parallels that in the degradation rate constants observed in B_{12} and related systems (such as cobalt porphyrins),[11] which increase for the more chlorinated congeners. What is noteworthy is the different reactivity of these catalysts toward *cis*- and *trans*-1,2-DCE: Our computed barriers for **TS16a** versus **TS16b** suggest that the enhanced degradation of *trans*-1,2-DCE over the *cis*-congener[11] may be rooted not only in the stabilities of the transient chlorovinylcobalt complexes but also in the kinetic parameters (activation barriers) leading to them.

The overall reaction profile for the parent reaction of $\mathbf{2}^-$ with PCE is summarized on the right-hand side of Figure 6 ($\Delta G(H_2O)$ level) and contrasted with that involving $\mathbf{3}^{\bullet-}$ as discussed in the previous section (left-hand side of Figure 6). We note the overall mutual compatibility of the two branches that we have

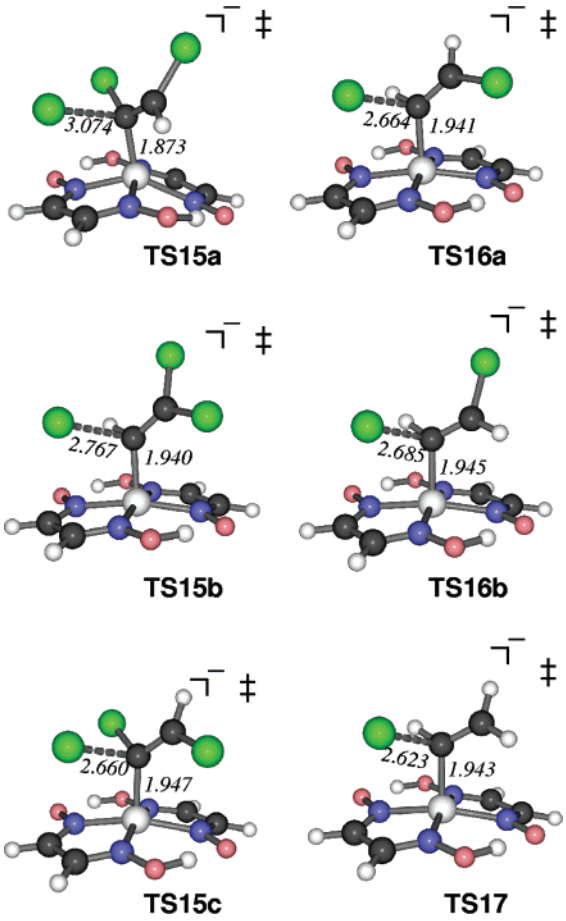

Figure 5. Transition states for chloride elimination involving other substrates, namely, PCE, *cis*-1,2-DCE, and VC for **TS15**, **TS16**, and **TS17**, respectively (in italics: BP86/AE1-optimized Co−C and C···Cl distances [in Å]).

Table 5. Relative Energies [kcal/mol] of the Chloride-Elimination Transition States in Figure 5 (+CH_2NH) with Respect to Separated Reactants (i.e., 2^- plus the respective chlorinated ethylene)[a]

	TS15a	TS15b	TS15c	TS16a	TS16b	TS17
ΔE(gas)	19.2	21.6	24.4	27.2	22.4	29.9
$\Delta E(H_2O)$	18.4	20.2	23.2	25.8	21.1	27.7
$\Delta G(H_2O)$	18.3	20.4	24.1	25.6	21.0	26.7

[a] BP86 level, AE2 single points on BP86/AE1-optimized geometries.

computed for these two quite different model systems. In both cases, i.e., for a methylated Co(II) radical ($\mathbf{3}^{\bullet-}$) and a diamagnetic Co(I) species ($\mathbf{2}^-$), viable pathways for reductive dehalogenation of chlorinated ethylenes in the coordination sphere of the metal have been identified, with formation of chlorinated vinylcobalt complexes via chloride dissociation as probable rate-limiting steps. Likewise, similar trends in the reactivity toward differently chlorinated substrates can be noted in both cases (i.e., TCE > PCE > DCE > VC). It is thus possible that the key characteristics of the rate-limiting transition states, namely, very long breaking C···Cl^- bonds in α position to the metal, may be transferable to other Co-based systems, and perhaps to the B_{12} family itself.

In Table 6, the electron distribution in the key stationary points of each branch, $\mathbf{4}^{\bullet-}$ and **TS13**−**14** for the alkylcobaloxim and Co(I) routes, respectively, is analyzed in terms of atomic NPA charges and spin distributions. In both cases, significant charge density is transferred to the PCE moiety, where it is accumulated on the C^α atom and on the leaving chloride in the case of $\mathbf{4}^{\bullet-}$ and **TS13**−**14**, respectively. In the radical anion, the unpaired electron is localized to a large extent on the C^β atom (see values in parentheses in Table 6).

Recently, an alternate mechanistic pathway for the dehalogenation process has been proposed for cob(I)alamins, namely, one involving chlorinated alkylcobalt complexes formed upon protonation,[13] e.g., for PCE:

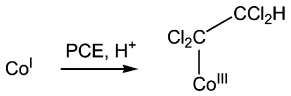

(16)

Under reductive conditions in solution, such alkyl complexes are indicated to be unstable with respect to dissociation into a Co(II) species, the dechlorinated alkene (TCE in the case of eq 16), and free chloride, thereby circumventing the intermediacy of vinyl complexes altogether.[13] For the model complexes in Figure 4, entry into this path would be possible by protonation of the alkene complex $\mathbf{13}^-$ affording an ethylcobaloxime derivative, $Co(Hgly)_2(-CCl_2-CCl_2H)$ (**18**); see Figure 7. If protonation of $\mathbf{13}^-$ would be clearly favored over chloride dissociation via **TS13**−**14**, the latter path would become less relevant. Indeed, a notable driving force, $\Delta G(H_2O) = -30.3$ kcal/mol, is computed for the reaction

$$\mathbf{13}^- + H_3O^+ \rightarrow \mathbf{18} + H_2O \qquad (17)$$

Thus, barring an unexpectedly high barrier for this process, this route would probably be favored in our dealkylated, base-off cobaloxime model. It should be noted, however, that accurate computation of acidity constants of aqueous transition-metal complexes (pertaining to the reverse of eq 17) is a difficult task.[51] What is more, a large part of the driving force for eq 17 stems from charge compensation, which should be less important in the cob(I)alamins with their different overall charge of the Co^I-corrin moiety (zero, as opposed to −1 in $\mathbf{13}^-$). To what extent this protonation route would be followed in the real systems is not fully clear at present. At this point we would like to emphasize the apparent feasibility of the nucleophilic attack mechanism sketched in the two branches of Figure 6 and the potential transferability to the biological systems. The question of whether there exist other, even more favorable pathways for the latter, such as the protonation route just discussed, clearly invites further studies.

For the actual cobaloximes, which are indicated to react via base-off alkylcobalt(II) radical anions, such a protonation route can probably be excluded. As detailed in section 3.2, the approach of the olefin to such a center ($\mathbf{3}^{\bullet-}$) already triggers the weakening of a C−Cl bond and the eventual loss of chloride thereof. The lifetime of transient species with strong Co−C interaction (such as $\mathbf{4}^{\bullet-}$, cf. Figure 2) is expected to be very short, probably too short for other intermolecular reactions.

Finally, we briefly address the possible competition between outer-sphere reduction of the olefins and the inner-sphere mechanisms discussed so far, taking PCE as a showcase example. One-electron reduction of PCE in solution is believed to yield an intermediate π^* radical anion in a first step.[8] Uptake of one electron by PCE is computed to be exothermic by −17.6 kcal/mol in the gas phase (ΔG)[52] and by −62.6 kcal/mol in water (ΔG), the latter value corresponding to a reduction

(51) Li, J., Fisher, C. L.; Chen, J. L.; Bashford, D.; Noodleman, L. *Inorg. Chem.* **1996**, *35*, 4694−4702.

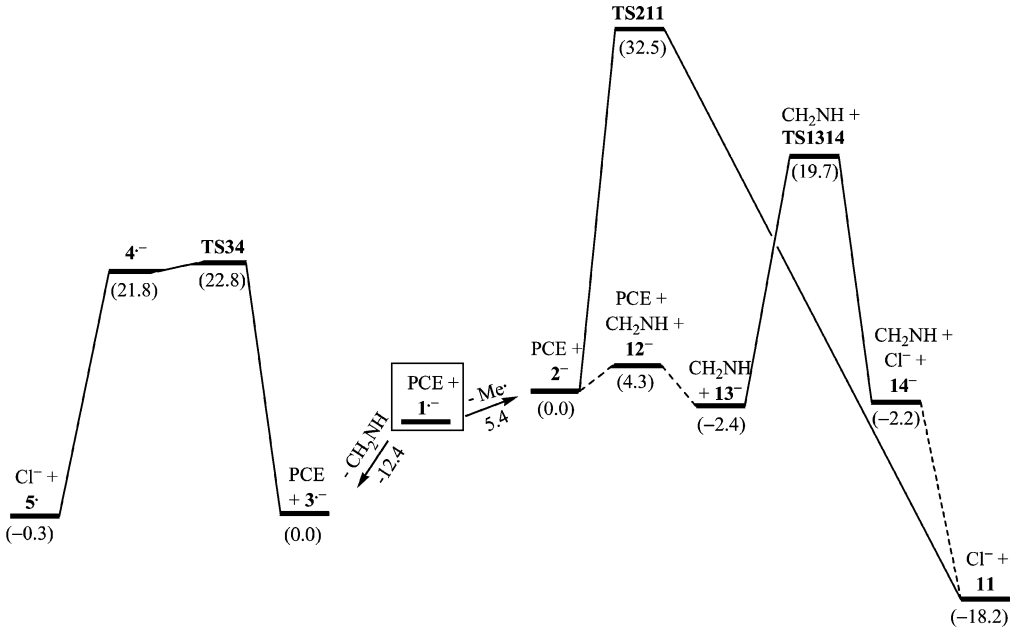

Figure 6. Schematic pathways for PCE addition to $\mathbf{3}^{\bullet-}$ (left-hand part) and $\mathbf{2}^{-}$ (right-hand part), as arising from the reduced cobaloxime $\mathbf{1}^{\bullet-}$ (central box); estimated $\Delta G(H_2O)$ values [in kcal/mol] are given relative to the respective resting states of a potential catalytic cycle in both branches.

Table 6. Selected Atomic Charges in Key Intermediates Involving Chloride Elimination from PCE (NPA data at the PCM(H_2O)/BP86/AE2 level, i.e., single-point calculations in a continuum; in parentheses: spin densities at the same level)

atom[a]	$\mathbf{4}^{\bullet-}$	TS13−14
Co	0.56 (0.02)	0.71
C^{α}	−0.36 (0.03)	−0.12
C^{β}	−0.17 (0.59)	−0.26
Cl*	−0.19 (0.17)	−0.74
Cl^{α}	−0.01 (0.00)	0.05
Cl^{β}(av)	0.06 (0.08)	0.06

[a] Cl* denotes the leaving chloride; the remaining atoms of the PCE moiety are labeled α or β according to their position relative to the metal (av denoting a mean value).

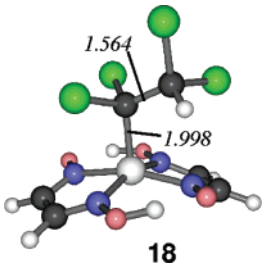

Figure 7. Protonation product of $\mathbf{13}^{-}$ (in italics: selected BP86/AE1-optimized distances [in Å]).

potential of −1.64 V.[53] Computed E^0 values for salient Co-based reductants are −1.33, −0.30, and −0.56 V for $\mathbf{1}/\mathbf{1}^{\bullet-}$ (Table 1), $\mathbf{3}/\mathbf{3}^{\bullet-}$ (section 3.2), and $\mathbf{2}^{\bullet}/\mathbf{2}^{-}$, respectively (−0.45 V for $\mathbf{12}^{\bullet}/\mathbf{12}^{-}$). Of these anions, only $\mathbf{1}^{\bullet-}$ would appear as a good candidate for promotion of outer-sphere reduction of PCE. The more stable "base-off" variant $\mathbf{3}^{\bullet-}$ is indicated to be a much less potent reductant, and the electron transfer according to

$$\mathbf{3}^{\bullet-} + \mathrm{PCE} \rightarrow \mathbf{3} + \mathrm{PCE}^{\bullet-} \qquad (18)$$

is highly endothermic, with computed $\Delta G(H_2O) = 31.0$ kcal/mol. The actual free-energy barrier[54] for this process would, arguably, be even higher. A similar result is obtained for the Co(I) species $\mathbf{2}^{-}$ or $\mathbf{12}^{-}$, indicating that the inner-sphere reductions discussed above can indeed be competitive with and even be more favorable than a simple outer-sphere pathway.[55]

4. Conclusions

We have applied modern DFT techniques to study key steps of reductive dehalogenation of chloroalkenes at cobalt centers arising from a model cobaloxime, $MeCo(Hgly)_2(NHCH_2)$ (Hgly = glyoximato). Two pathways were considered after initial one-electron reduction of this complex, affording either a methylated Co(II) species, $[MeCo(Hgly)_2]^{\bullet-}$, or a Co(I) complex, $[Co(Hgly)_2(NHCH_2)]^{-}$. The former would be the preferred route for the model cobaloxime, whereas the latter should model the corresponding chemistry of the related cobalamins. Both anions can react with chloroethenes $ClCX_1{=}CX_2X_3$, producing vinylcobalt complexes with a $Co{-}CX_1{=}CX_2X_3$ moiety (X = Cl or H). Formation of these vinyl complexes under elimination of chloride is indicated to be the rate-limiting steps in potential catalytic cycles, with computed free energies of activation on the order of 20 kcal/mol. This is the first computational evidence

(52) ΔE(gas) = −13.5 kcal/mol, similar to values for the gas-phase electron affinity that have been obtained in experiments and DFT and ab initio calculations: (a) Chen, E. C. M.; Wiley, J. R.; Batten, C. F.; Wentworth, W. E. *J. Phys. Chem.* **1994**, *98*, 88−94. (b) Bylaska, E. J.; Dupuis, M.; Tratnyek, P. G. *J. Phys. Chem. A* **2005**, *109*, 5905−5916.

(53) A somewhat more negative value, −1.98 V, has been derived empirically in ref 8.

(54) For the computation of such barriers in electron-transfer processes see for example: (a) Rosso, K. M.; Rustad, J. R. *J. Phys. Chem. A* **2000**, *104*, 6718−6725. (b) Rosso, K. M.; Dupuis, M. *Theor. Chem. Acc.* **2006**, *116*, 124−136.

(55) For the radical anions of the other chlorinated olefins, no corresponding π^* states could be located, and only σ^* states (i.e., loose complexes between chlorinated vinyl radicals and Cl^{-}) were found (also at restricted-open-shell DFT levels, cf.: Bylaska, E. J.; Dupuis, M.; Tratnyek, P. G. *J. Phys. Chem. A* **2005**, *109*, 5905−5916). For these σ^* states, the computed reduction potentials of TCE, *cis*-DCE, and VC are −1.36, −1.67, and −1.83 V, respectively. In all cases, outer-sphere reduction of these olefins would appear less favorable than the inner-sphere mechanisms (cf. ΔG values in Table 3).

that reductive dechlorination can follow an inner-sphere mechanism, i.e., that it can occur in the coordination sphere of the metal. The computed reduction potentials of the putative active catalysts and a typical substrate, perchlorethylene, also suggest that these inner-sphere reactions are more facile than direct, outer-sphere reduction. Despite the very different nature of the Co species involved in the two inner-sphere branches studied, similar trends in the rate-determining barriers are predicted as the olefin is varied, suggesting a certain transferability of the key aspects of this process to other cobalt species as well.

For the Co(I) model species it turns out that attack on the olefin is most likely preceded by dissociation of the base and formation of a transient η^2-olefin complex. This finding has important implications for the mechanism of a functional biological system based on vitamin B_{12}, which is also believed to be active in the form of the four-coordinate "supernucleophile" cob(I)alamin. For the model system it appears that the base has to coordinate again to the metal after attack on the olefin in order to shift the equilibrium toward the product side. Hence, a base that is tethered to the metal complex (as in the actual B_{12} cofactor) could be quite effective in a "base-on/base-off" switching mechanism.

The transient η^2-perchlorethylene complex in the anionic model system is computed to be readily protonated, affording a chlorinated ethylcobalt(III) derivative akin to those proposed recently to be involved in an alternative path for reductive dehalogenation with cobalamins and vitamin B_{12}. Further studies of these competing pathways should be directed toward the role of the ancillary ligands at the metal.

Acknowledgment. This work was supported by the Deutsche Forschungsgemeinschaft. M.B. thanks Prof. Walter Thiel and the Max-Planck society for support, and unknown referees for helpful comments. Computations were performed on Compaq XP1000, ES40, and Intel Xeon workstations and PCs at the MPI Mülheim.

Supporting Information Available: BP86/AE1-optimized geometries of all Co complexes discussed in the text (Cartesian coordinates in *xyz* format) and full author list of ref 33 are available free of charge via the Internet at http://pubs.acs.org.

OM070027S